Biochimica et Biophysica Acta 1842 (2014) 1109–1120

Contents lists available at ScienceDirect

Biochimica et Biophysica Acta

journal homepage: www.elsevier.com/locate/bbadis

Negatively regulating TLR4/NF-κB signaling via PPARα in endotoxin-induced uveitis

Wei Shen [a], Yang Gao [a,b], Boyu Lu [b], Qingjiong Zhang [b], Yang Hu [c,*], Ying Chen [a,**]

[a] Department of Physiology, University of Oklahoma Health Sciences Center, Oklahoma City, OK, USA
[b] State Key Laboratory of Ophthalmology, Zhongshan Ophthalmic Center, Sun Yat-sen University, Guangzhou, PR China
[c] Arthritis and Clinical Immunology Research Program, Oklahoma Medical Research Foundation, Oklahoma City, OK, USA

ARTICLE INFO

Article history:
Received 6 September 2013
Received in revised form 27 March 2014
Accepted 31 March 2014
Available online 6 April 2014

Keywords:
Endotoxin induced uveitis
LPS
TLR4
PPARα

ABSTRACT

Toll-like receptor (TLR) signaling plays a fundamental role in the induction and progression of autoimmune disease. In the present study, we showed that lipopolysaccharide (LPS), a TLR4 ligand, functions as an antagonist of peroxisome proliferator-activated receptor alpha (PPARα), a nuclear transcription factor. Using endotoxin induced uveitis (EIU) as a model, we found that TLR was negatively regulated by PPARα. Our data revealed that treatment with the PPARα agonist fenofibrate dramatically prevented LPS-induced uveitis and inhibited TLR/Nuclear factor-kappaB (NF-κB) signaling during inflammation. Evaluation of the severity of anterior uveitis further showed that PPARα agonist treatment significantly decreased inflammatory cell infiltration, total protein concentration, vessel density, inflammatory cytokine production, and clinical scores in the anterior section of the eye during EIU. Moreover, fenofibrate administration recovered retinal function and decreased the production of inflammatory cytokines, retinal vascular leukostasis, and inflammatory cell infiltration into the posterior section of the eyes during EIU. In vitro studies further showed that down-regulation or deletion of PPARα led to increased TLR4 levels and the activation of NF-κB signaling in RPE cells and also blocked the anti-inflammatory effects of fenofibrate. Furthermore, activation or up-regulation of PPARα decreased TLR4 levels and inhibited the NF-κB signaling pathway induced by LPS in RPE cells. In TLR4-expressing reporter cells, activation or up-regulation of PPARα partially inhibited the activation of NF-κB and also decreased TLR4 transcriptional activity. In conclusion, the activation of PPARα represents a novel therapeutic strategy for human uveitis, as PPARα negatively regulates TLR4 activity and therefore exerts anti-inflammatory actions.

Published by Elsevier B.V.

1. Introduction

The Toll-like receptors (TLRs) constitute a family of recently discovered innate immune recognition receptors, which play fundamental roles in the induction of innate immunity, inflammation, cell survival, and proliferation. The activation of TLR signaling is mediated through the binding of various ligands, including lipids, lipoproteins, proteins, and nucleic acids derived from bacteria, viruses, and fungi. Thus far, 10 TLRs have been identified in humans and 12 functional TLRs in mice, and TLR1 to TLR9 are highly conserved in both humans and mice [1,2]. The best-studied member of the TLRs is TLR4, which is primarily associated with the accessory protein MD-2 and the co-receptor CD14 to recognize lipopolysaccharide (LPS), a glycolipid component of the outer membrane of Gram-negative bacteria. LPS recognition then activates the Toll/IL-1R (TIR) domain-containing adaptor molecule MyD88 (myeloid differentiation factor 88)-dependent pathway [3,4]. TLR4 is expressed on the cell surface and cycles between the Golgi and the plasma membrane in both immune cells, such as monocytes/macrophages, and nonprofessional immune cells, such as epithelial cells [4–6]. The expression of TLR4 plays a pivotal role in host defense, and inappropriate TLR4 activation can result in the acceleration of inflammatory and autoimmune diseases.

One example of aberrant TLR4 activation is LPS-induced endotoxin induced uveitis (EIU), a widely used experimental induction of uveitis for studying the mechanisms of innate inflammation and for validating potential therapeutic modalities for human uveitis, which constitutes an ocular emergency and is one of the leading causes of legal blindness in the US [7–9]. Experimental induction of EIU is achieved through subcutaneous injection with one dose of LPS, which specially targets the uvea-resident tissues consisting of pigmented epithelial cells and the vascular cells of the eye. Injection of LPS results in TLR4 signaling in cooperation with MyD88 to activate NF-κB, culminating in potent

Abbreviations: EIU, endotoxin induced uveitis; EAU, experimental autoimmune uveitis; ICAM-1, intercellular adhesion molecule-1; LPS, lipopolysaccharide; MyD88, myeloid differentiation factor 88; NF-κB, nuclear factor-kappaB; PPARs, peroxisome proliferator-activated receptors; shRNA, small hairpin RNA; TIR, Toll/IL-1R; TNF-α, tumor necrosis factor-alpha; VEGF, vascular endothelial growth factor

* Correspondence to: Y. Hu, Oklahoma Medical Research Foundation, Oklahoma City, OK 73104, USA.
** Correspondence to: Y. Chen, 941 Stanton L. Young Blvd., BSEB 313, Oklahoma City, OK 73104, USA. Tel.: +1 405 271 8001x42401.
E-mail addresses: yang-hu@omrf.org (Y. Hu), ying-chen@ouhsc.edu (Y. Chen).

http://dx.doi.org/10.1016/j.bbadis.2014.03.015
0925-4439/Published by Elsevier B.V.

transcription of inflammatory cytokines [10]. Down-regulation of TLR4 mRNA could contribute to endotoxin tolerance, whereas the lack of TLR4 in rodents has resulted in resistance to EIU [4,11,12].

Peroxisome proliferator-activated receptor alpha (PPARα) is a transcription factor that is highly expressed in vascular cells and pigment cells. In addition to controlling the expression of genes involved in lipid metabolism, recent studies have found that activation of PPARα ameliorates inflammation by inhibiting NF-κB activity [13,14], suppressing pro-inflammatory cytokine production [15,16], and modulating endothelial neutrophil production [17]. Despite these findings, the precise mechanism responsible for these effects of PPARα and its relationship with TLR4 remains obscure.

Using the model of EIU, we evaluated the therapeutic importance of PPARα activation for LPS-induced uveitis, and we found that PPARα acts as a TLR4 repressor by inhibiting TLR4 transcription and that, contrary to its role as a TLR4 activator, LPS acts as a PPARα antagonist. Thus, the manner in which LPS induces TLR4 transcription is through the inhibition of PPARα, and our study therefore provided a novel mechanistic insight into TLR signaling in auto-inflammatory diseases.

2. Materials and methods

2.1. Animals

All animal experiments were conducted in strict agreement with the Association for Research in Vision and Ophthalmology (ARVO) Statement for the use of Animals in Ophthalmic and Vision Research. Adult male Lewis rats (age range, 8–10 weeks; weight range, 150–200 g) were purchased from Charles River (Wilmington, MA) and kept in 12 h light/12 h dark cycle in the animal facility at the University of Oklahoma Health Science Center (Oklahoma City, OK).

2.2. Endotoxin-induced uveitis

Lewis rats (Charles River Laboratories, Wilmington, MA), 10 week old, were randomly distributed into three groups (12 rats each group) and were subcutaneously injected with 200 μg LPS (Sigma-Aldrich, St. Louis, MO) into their hindback. All the rats were euthanized 24 h after LPS injection. For fenofibrate treatment group, rats were fed a chow containing with fenofibrate (120 mg/kg/d) for 7 days and followed with the EIU induction.

2.3. Clinical evaluation of EIU

Slit lamp examination was conducted 24 h after the LPS injection before the euthanization. Pictures of the anterior part reflecting the visualization were taken by the handle hold retina camera (Kowa, Japan). Clinical scoring of the EIU was performed as follows [18]: the severity of the EIU was graded from 0 to 4 using the scale: 0 = no inflammatory reaction; 1 = discrete inflammation of the iris and conjunctival vessels; 2 = dilation of the iris and conjunctival vessels with moderate fare in the anterior chamber; 3 = hyperemia in iris associated with Tyndall effect in the anterior chamber; 4 = same clinical signs as 3 plus the presence of fibrin or syncehiae.

2.4. Induction of experimental autoimmune uveitis (EAU)

Male Lewis rats at age of 10 weeks were immunized by subcutaneous (hindback) injection with a single dose of 50 μg recombinant human retinal soluble antigen (SAg) peptide S35 (341–360) (AnaSpec Inc., San Jose, CA), emulsified with complete Freund's adjuvant (1:1 w/v) (Sigma-Aldrich, St. Louis, MO) and supplemented with pertussis H37Ra at 2.5 mg/ml (Difco, Detroit, MI). Controls were injected with the same amount of CFA, emulsified with saline (200 μl per rat). The severity of the disease was inspected by slip lamp starting from the 7th day following immunization. Twenty one days after immunization, the rats were euthanized and the eyes were collected for experiments. For fenofibrate treatment group, rats were pre-fed a chow containing with fenofibrate (120 mg/kg/d) for 1 day and then 21 days right after the induction.

2.5. Electroretinogram (ERG) recording

ERG was recorded with a gold electrode placed on the cornea, a reference electrode in the mouth, and a ground electrode on the tail. Dark adaptation was for 12 h and the light adaptation was for 5 min. The flash intensities for scotopic and photopic ERG were 1000 and 2000 $cd \cdot s/m^2$, respectively. The ERG waveforms of both eyes in the same animal were simultaneously recorded.

2.6. Histopathologic evaluation of EIU

After the euthanization, the eyes were nucleated immediately and stored in 4% PFA solution at 4 °C and embedded in paraffin. The 10-μm sagittal sections were cut through the nerve and stained with hematoxylin and eosin. For histopathologic evaluation, the anterior and posterior chambers were examined with the light microscopy.

2.7. Cell infiltration and protein concentration in aqueous humor

Aqueous humor was collected by anterior chamber puncture with an insulin syringe immediately after the euthanization of the rats. For the cell counting, 1 μl of aqueous humor was diluted in 9 μl PBS and then suspended with 10 μl Trypan blue solution, and the cells were counted with a hemocytometer under the light microscopy. The number of cells per field (an equivalent of 0.1 μl) was obtained by averaging the results of four fields from each sample. The total protein concentration in the aqueous humor was measured by Coomassie Blue assay. The aqueous humor samples were centrifuged at 2500 rpm for 5 min at 4 °C to obtain the supernatant. All the aqueous humor samples were stored in the ice until tested, and cell counts and total protein concentration were measured on the day of sample collection.

2.8. Evaluation of retinal vascular adherent leukocytes

Leukocyte adhesion to the retinal vessels was evaluated 24 h after EIU induction. Briefly, rats were anesthetized and perfused through the left ventricle with PBS to remove circulating leukocytes in blood vessels. The adherent leukocytes in the vasculature were stained by perfusion with FITC-conjugated concanavalin-A (Con-A; 40 μg/ml, Vector Laboratories, Burlingame, CA). The eyes were removed and fixed in 4% paraformaldehyde. The retinas were dissected and flat-mounted. Adherent leukocytes in the retinal vasculature were counted under a fluorescence microscope.

2.9. Cell culture and primary cell culture

ARPE 19 cells were cultured in a DMEM medium containing 10% Fetal Bovine Serum and 1% Ampicillin. At confluence of 95%, cells were exposed to 1 μg/ml LPS in the presence or absence of 50 μM fenofibrate, 10 μM GW6471 (Sigma, St. Louis, MO) or 50 μM WY 14643 (Sigma, St. Louis, MO) for 24 h. For primary cell culture, tissues isolated from C57/BL6 and *Pparα*$^{-/-}$ mice (3–4 week old) were minced, digested, plated and cultured in DMEM medium containing 5% FBS, 1% antibiotics, 1% no essential amino acid, 1% insulin transferrin selenium and 20 mM HEPES.

2.10. Immunohistochemisty

Immunohistochemistry was followed a procedure as described previously [19]. Antibodies: mouse anti-NF-κB (1:100, Abcam, Cambridge, MA), rabbit anti-TLR4 antibody (1:100, Abcam, Cambridge,

MA), Alexa Fluor 568 goat anti-mouse IgG (H + L), and Alexa Fluor 488 goat anti-rabbit IgG (H + L) (1:100, Invitrogen, Eugene, OR).

2.11. Western blotting analysis

Western blotting analysis was followed a procedure as described previously [19]. The antibodies are: rabbit anti-phosphorylated-NF-κB (1:1000, Santa-Cruz Biotechnology), mouse anti-TLR4 (1:1000, Abcam, Cambridge, MA), rabbit anti-ICAM-1 (1:500, Cell Application, San Diego, CA), rabbit anti-TNF-α (1:500, Cell Application, San Diego, CA), rabbit anti-VEGF (1:1000; Santa-Cruz Biotechnology, Santa-Cruz, CA), rabbit anti-MCP-1 (1:500; Abcam, Cambridge, MA), rabbit anti-TLR4 antibody (1:1000, Abcam, Cambridge, MA), and mouse anti-β-actin (1:5000; Sigma-Aldrich, St. Louis, MO).

2.12. Quantitative real-time reverse transcription (RT)-PCR

Quantitative real-time PCR was followed a procedure as described previously [19]. TLR-4 primers: 5′-AGAACTGCAGGTGCTGGATT-3′ and 3′-AAACTCTGGATGGGGTTTCC-5′.

2.13. Construction of the TLR4 promoter

A segment containing 500 bp of upstream and 100 bp of downstream sequence relative to the predicted transcription start site (TSS) of the human TLR4 gene was amplified by a PCR from human genomic DNA. The amplified promoter fragments were digested with the appropriate restriction enzymes (New England Biolabs, Ipswich, MA) and cloned into the reporter gene expression vector pGLuc-04 (Promega, Madison, WI), which contains a Firefly luciferase reporter gene downstream from the multiple cloning sites.

2.14. TLR4 promoter activity assay

ARPE19 cells (1×10^4 cells/well of 24-well dish) were co-transfected with 0.1 μg p-human TLR4 promoter-Luc and 20 ng Renilla luciferase expression vector pGL4.75 (Promega, Madison, WI) as an internal control by lipofection. Twenty-four hours after achieved optimal efficiency, cells were cultured in a medium containing with or without WY14643 (50 μM) and GW6471(10 μM) for 24 h and then exposed to LPS (1 μg/ml) for 1 h. Luciferase activities of each group cells were measured by using the Dual-Luciferase Reporter Assay System Kit (Promega, Madison, WI).

2.15. Monitoring NF-κB activation

At a confluence of 90%, ARPE19 cells were transfected with a vector carrying an inducible secreted embryonic alkaline phosphatase (SEAP) reporter gene, which was under the control of an ELAM-1 (E-selectin) promoter fused to five NF-κB and AP-1-binding sites (Invivogen, San Diego, CA). Forty-eight hours after transfection, the cells were exposed to a culture medium containing with or without various ranges of fenofibrate, WY14643 or GW6471 overnight and then exposed to 0.1 ng/ml LPS-EB Ultrapure (Invivogen, San Diego, CA) for 1 h. Levels of SEAP (indicating the NF-κB and AP-1 activities) were detected and quantified by Quanti-Blue following manufacturer's protocols (Invivogen, San Diego, CA).

HEK293 reporter cells with stably expressed human TLR4, MD-2 and CD14 co-receptor genes, and an inducible SEAP reporter gene controlling an IL-12 p40 minimal promoter fused to five NF-κB and AP-1-binding sites were stimulated with a range of fenofibrate (0–100 μM) for 24 h and 0.1 ng/ml LPS-EB for another hour. Levels of SEAP were detected and quantified by Quanti-Blue following manufacturer's protocols (Invivogen, San Diego, CA).

C3H/TLR4mut reporter cells were generated from TLR4-deficient murine embryonic fibroblasts and stably express an NF-κB inducible SEAP reporter gene (Invivogen, San Diego, CA) and were served as control in this study. The mutant reporter cells were stimulated with 0.1 ng/ml TLR2 and TLR3 agonists and LPS-EB in the presence of a range of fenofibrate orWY14643 at a concentration of 50 μM. Levels of SEAP was detected and quantified by Quanti-Blue following a manufacture protocols (Invivogen, San Diego, CA).

2.16. PPARα activity assay

The responsive reporter cells which expressed the encoding human NR1C1 gene (PPARα) and luciferase were dispensed into 96 wells (5×10^3 cells/well) of assay plate and exposed to a medium containing various ranges of GW590735 (0–100 nM) or WY14643 (0–100 μM) to reach an effective concentration value. At a value of EC_{50}, the reporter cells were exposed to LPS at different doses (0–4 ng/ml) overnight following manufacturer's protocol (Indigo Bioscience, PA). The luciferase activities were quantified by the intensity of light emission from each sample using a luminometer.

2.17. Statistical analysis

Data were presented as mean ± SD. Statistical analyses were performed using the Mann–Whitney *U* test or *ANOVA* test. A *p*-value < 0.05 was considered as statistically significant.

3. Results

3.1. PPARα agonist inhibited ocular inflammation in EIU and EAU rat models

Firstly, we examined whether fenofibrate was capable of ameliorating the ocular inflammation and rescuing retinal function during EIU. Adult Lewis rats were pre-fed with fenofibrate for 1 week and then injected with LPS to induce EIU. Twenty-four hours following the induction, the severity of EIU was evaluated. LPS injection induced an average clinical inflammation score of ~2.8 ($p < 0.001$ vs. control). Treatment with fenofibrate significantly reduced the clinical score to 1.2 ($p < 0.01$, Fig. 1A & B). Quantitative analysis for the inflammatory cellular infiltration and protein leakage in the Aqueous Humor (AqH) showed 118 ± 22.93 × 10^5 cells/ml ($p < 0.001$ vs. controls 0) (Fig. 1C) and 6.3397 ± 0.07 mg/ml leakage protein ($p < 0.01$ vs. controls 2.86428 ± 0.753 mg/ml) (Fig. 1D) in EIU rats, which was significantly reduced by oral fenofibrate to 10.07 ± 2.8 × 10^5 cells/ml ($p < 0.0001$ vs. EIU) (Fig. 1C) and 1.944 ± 0.923 mg/ml ($p < 0.001$ vs. EIU) (Fig. 1D), respectively.

We investigated the effect of fenofibrate on monocyte chemoattractant protein (MCP)-1, a chemokine which plays crucial role in the induction of EIU, and VEGF, a major angiogenic factor for vascularization and a key mediator for increased vessel permeability to cause protein leakage, in anterior segment of the eye. LPS induction dramatically increased in AqH MCP-1 and VEGF and the increases were suppressed by fenofibrate to a level comparable to the controls (Fig. 1E and 1F). Histopathologic analysis of the cell infiltration showed high cell infiltration in anterior and posterior segments of the eye from rats during EIU, and treatment with fenofibrate reduced the cell infiltrations (Fig. 1G). Immunohistochemistry study of NF-κB demonstrated an intensive signal in the anterior eye from EIU rats and a weak signal from controls and EIU rats treated with fenofibrate (Fig. 1H).

We examined the effect of fenofibrate on leukostasis, an early process of inflammation whereby inflammatory cytokines transmigrate into tissues, during EIU. As shown in Fig. 2A and B, LPS injection resulted in leukocyte attachment to the endothelial cells of retina, which was potently suppressed by pre-treatment with fenofibrate. During EIU, levels of VEGF and MCP-1 were remarkably increased in the eyecups and treatment with fenofibrate significantly prevented the release of these inflammatory markers (Fig. 2C and D). The effects of fenofibrate on retinal functions were examined by ERG. Compared with the controls,

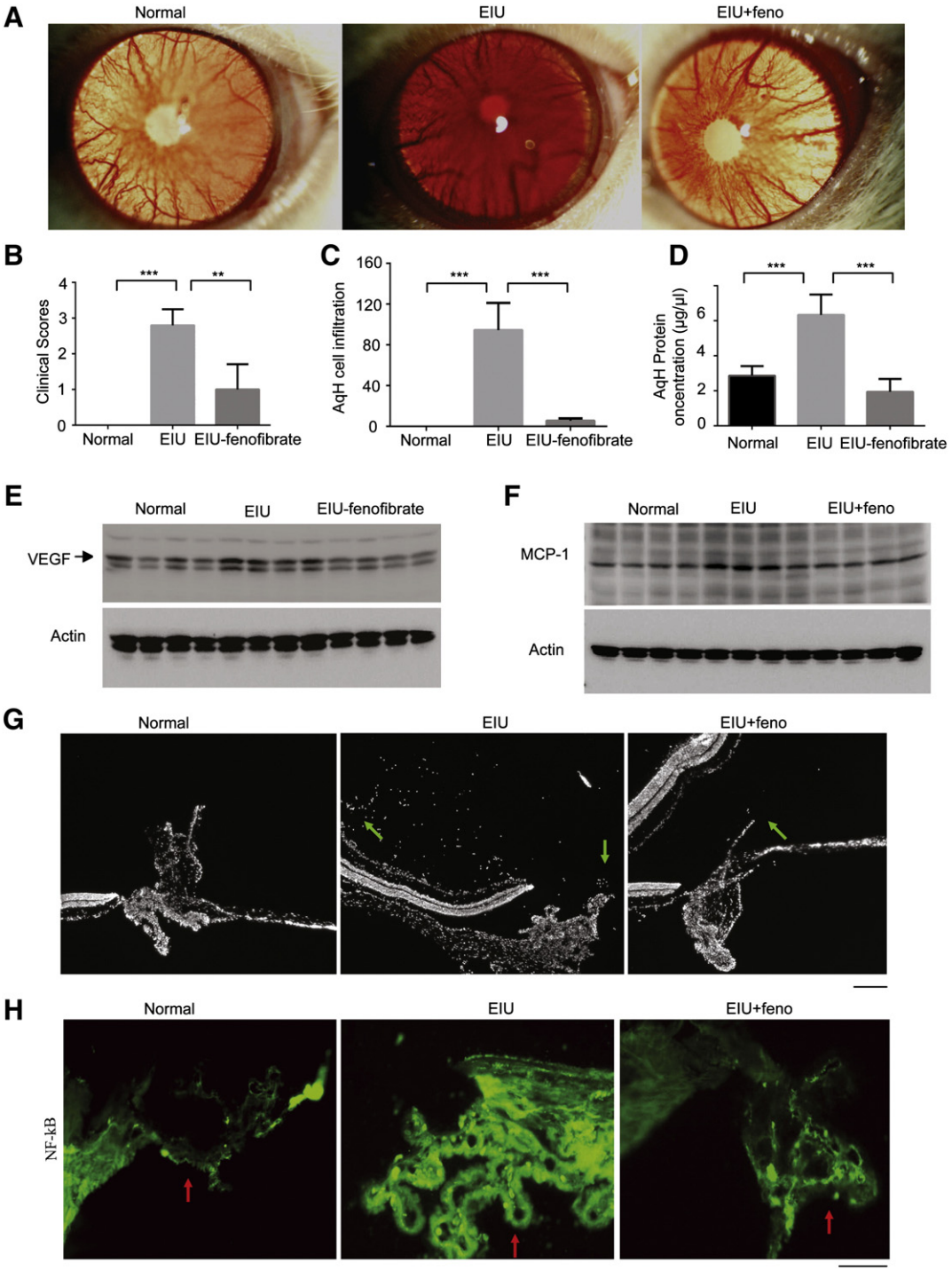

Fig. 1. Therapeutic potential of PPARα agonist on anterior eye during EIU. Adult Lewis rats were pre-treated with fenofibrate (120 mg/kg/d) for 7 days and then induced EIU with LPS. Twenty-four hours following induction, the rats were subjected for studies. A: Representative ocular photography was taken at 24 h following induction. B: Clinical inflammatory scores of EIU in Lewis rats in the absence or presence of fenofibrate were determined at 24 h after LPS injection. C: Cell infiltrations in the anterior chamber (AqH) of the EIU rats with or without fenofirate pre-treatment. D: Total protein in AqH was measured and compared (B–D, Mann–Whitney *U* test was used for analysis. Normal: $n = 6$; EIU: $n = 7$; EIU-fenofibrate: $n = 7$, $^{**}p < 0.05$, $^{***}p < 0.001$). E & F: Western blot analysis of MCP-1 and VEGF in AqH from rats of control, EIU and EIU pretreated with fenofibrate. Each lane presents one individual animal. G: Representative ocular sections were from normal rats, EIU rats, and EIU rats pre-treated with fenofibrate. Scale bar: 50 μM. H: Representative immunocytochemical staining of NF-κB in the anterior segment of the eyes from normal rats, EIU rats, and EIU rats pre-treated with fenofibrate. Scale bar: 20 μM.

EIU rats exhibited a significantly suppressed scotopic ERG during EIU at a level approximately 60% in A wave and 40% in B wave of that in age-matched control rats ($p < 0.05$ vs. normal) (Fig. 2E), suggesting compromised rod functions. Feeding with fenofibrate returned the decreased A wave and B wave to the approximate levels of 70% and 80% in control rats, respectively ($p < 0.05$ vs. EIU rats without fenofibrate treatment) (Fig. 2E), indicating a rescuing effect of fenofibrate on rod functions. In all EIU groups, both A wave and B wave amplitudes in photopic ERG were not significantly changed compared with the control group.

The anti-inflammation effects of fenofibrate on EAU were examined in rats immunized with human SAg peptide as well. Ocular histopathology examination in normal rats, EAU rats, and EAU rats treated with fenofibrate on day 21 revealed severe photoreceptor destruction and retinal disorganization in EAU rat, which was completely prevented by

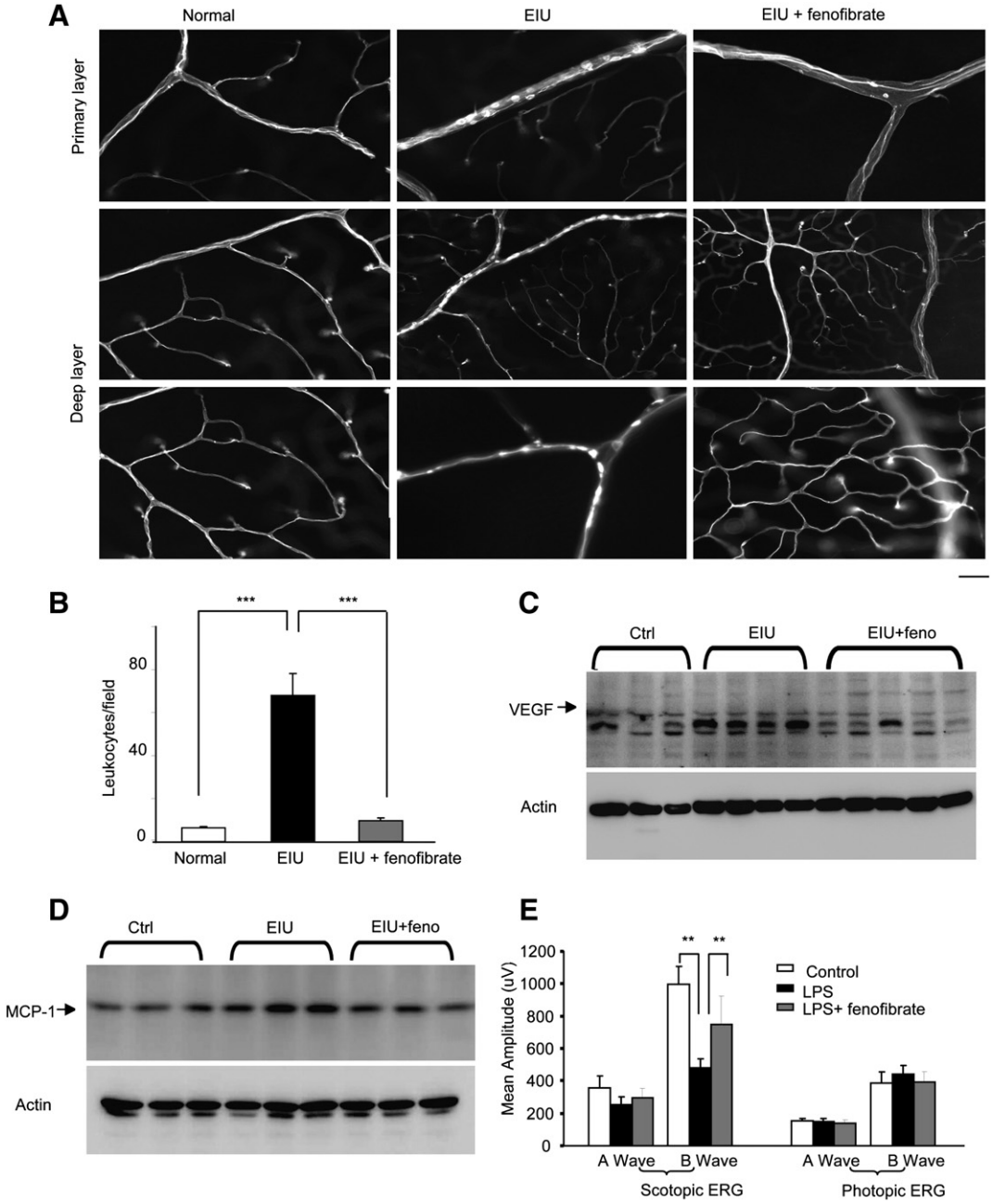

Fig. 2. Therapeutic potential of PPARα agonist on posterior eye during EIU. A: Retinal vascular endothelial cells and adherent leukocytes were stained with FITC conjugated Con-A (green) in normal rats, EIU rats, and EIU rats pre-treated with fenofibrate after the circulating leukocytes were removed by perfusion. The retinae were flat-mounted, and the adherent leukocytes were visualized and calculated. Scale bar: 20 μM. B: Multiple leukocytes adherent to endothelium of retinal vasculature were observed in the retina from EIU rats but not in the normal rats. Feeding with fenofibrate reduced the leukocytes attachments (mean ± SD, $n = 4$, $^{**}p < 0.01$). C–D: The levels of VEGF and MCP-1 in the eyecups from normal rats, EIU rats, and EIU rats pre-treated with fenofibrate were determined by Western blot analysis and normalized by β-actin levels. E: Statistic scotopic and photopic ERG showed the changes of B wave in scotopic ERG in normal rats, EIU rats, and EIU rats pre-treated with fenofibrate (mean ± SD, $n = 3$, $^{**}p < 0.01$).

daily oral fenofibrate administration (Supplemental Fig. 2A). Analysis of retinal inflammatory cytokines indicated high levels of TLR4, iris and vitreous VEGF, MCP-1, TNF-α, and NF-κB in EAU rats but not in normal rats and EAU rats treated with fenofibrate (Supplemental Fig. 2B). These results support the finding that fenofibrate has a therapeutic potential for ocular inflammation.

3.2. The PPARα agonist fenofibrate attenuated LPS-induced cytokine production and inhibited NF-κB signaling in RPE cells

RPE cells express a variety of cytokines and adhesion molecules, which contribute to the inflammatory response of the retina and maintain the eye as an immune-privileged site. Given that PPARα agonists are capable of preventing the ocular inflammation induced by LPS in vivo, we examined whether the PPARα agonist fenofibrate could inhibit the production of inflammatory cytokines involved in downstream LPS/TLR4 signaling in RPE cells. ARPE19 cells were exposed to LPS and were treated with fenofibrate or with vehicle as a control. The cellular levels of tumor necrosis factor alpha (TNF-α), which is induced and released upon LPS binding to TLR4, and ICAM-1, which can be stimulated by both LPS and TNF-α, were assessed using Western blotting. As shown in Fig. 3, exposure to LPS stimulated significant increases in TNF-α ($p < 0.01$ vs. vehicle, Fig. 3A and C) and ICAM-1 ($p < 0.01$ vs. vehicle, Fig. 3B and D), which were significantly reduced

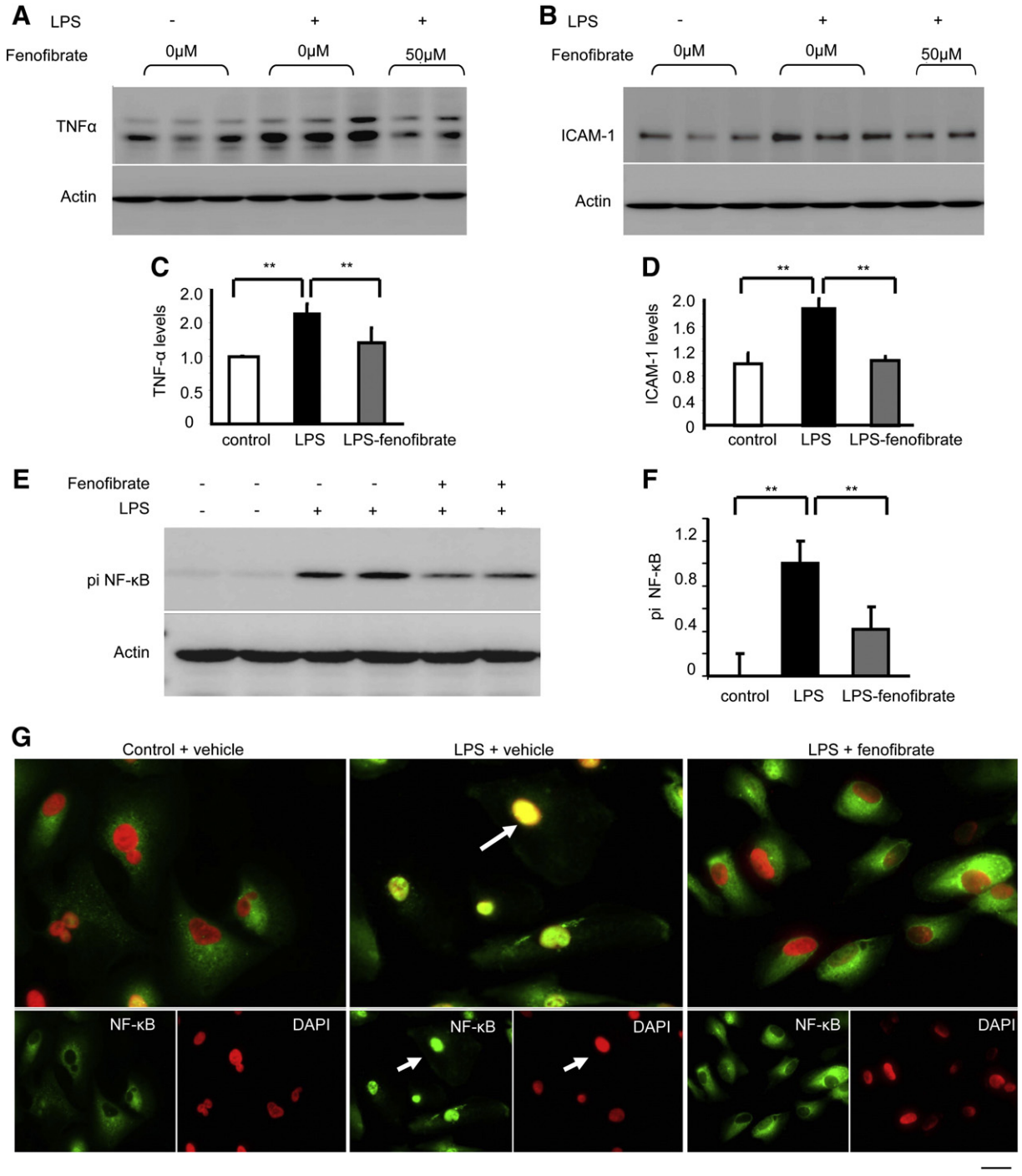

Fig. 3. PPARα agonists attenuated LPS-induced cytokine production and inhibited NF-κB activation in RPE cells. Confluent RPE cells were cultured in the absence or presence of 50 μM fenofibrate for 24 h and exposed to 1 μg/ml LPS for 1 h. A–F: Representative blots analysis of cellular TNF-α, ICAM-1, and phosphorylated NF-κB levels in the whole cell lysis from RPE cells. Semi-quantified by densitometry and normalized by β-actin (mean ± SD, $n = 5$, $^{**}p < 0.01$). G: Representative immunocytochemical analysis of the effect of fenofibrate on NF-κB nuclear translocation in RPE cells exposed to LPS. Scale bar: 20 μm in upper panel and 50 μm in lower panel.

in response to fenofibrate at a concentration of 50 μM ($p < 0.01$ vs. LPS, Fig. 3A–D).

To assess the role of fenofibrate in LPS/TLR4 signaling more accurately, we examined NF-κB nuclear translocation and phosphorylation, which both serve as indicators of downstream signaling following TLR4 activation. Exposure of RPE cells to LPS elevated NF-κB phosphorylation and induced NF-κB nuclear translocation, and these effects were fully reversed by the co-application of fenofibrate at a concentration of 50 μM (Fig. 3E–H, arrows in Fig. 3H showing NF-κB nuclear translocation).

3.3. PPARα agonist treatment suppressed TLR4 expression and inhibited TLR4 signaling

To further confirm the specificity of fenofibrate on TLR4/NF-κB signaling, RPE cells were transiently transfected with a vector expressing MD-2 and the secreted embryonic alkaline phosphatase (SEAP) reporter gene under the control of NF-κB. These cells then were stimulated with LPS in the presence of fenofibrate or vehicle, and activation of TLR4 signaling was measured according to SEAP activity. LPS exposure induced

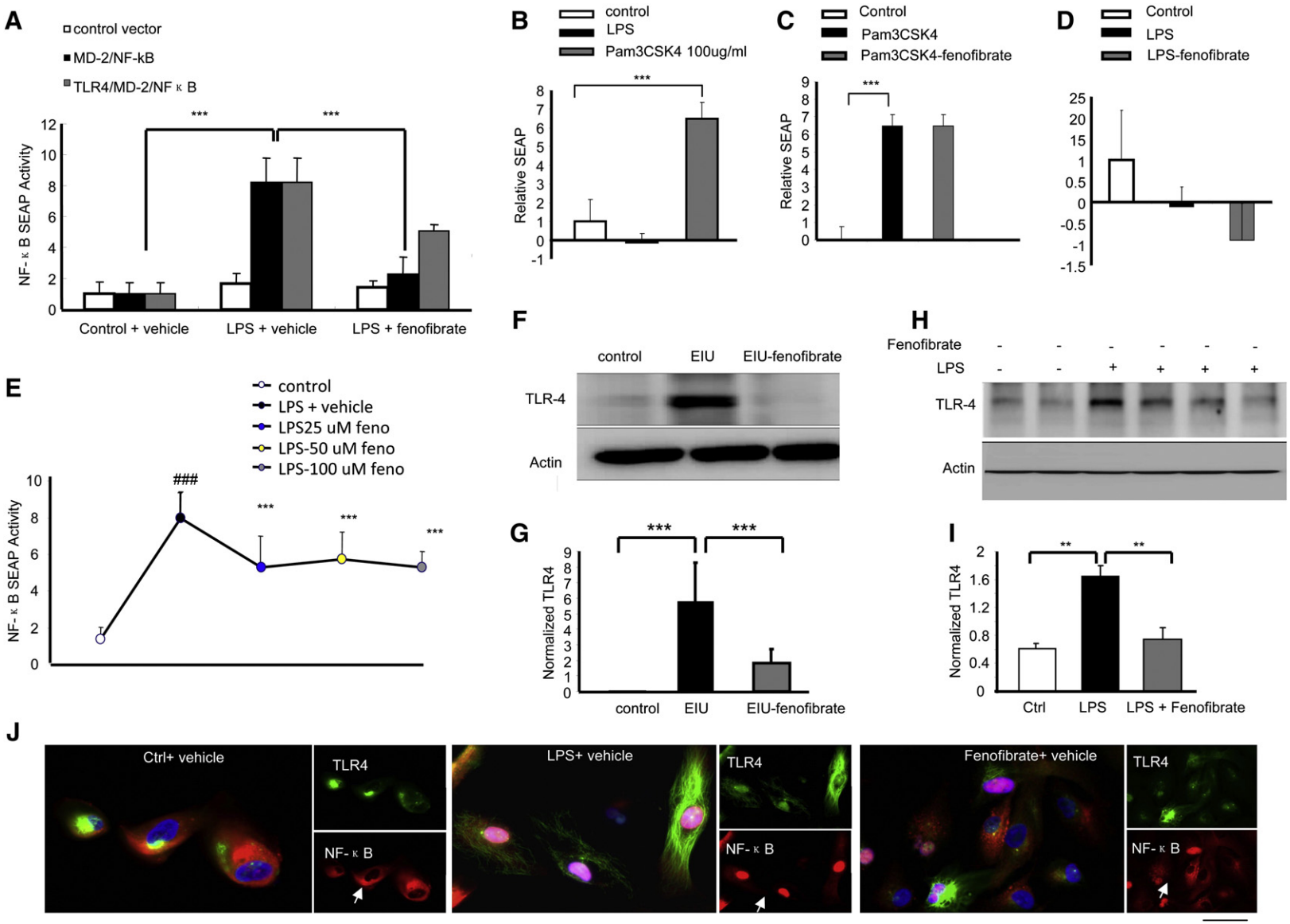

Fig. 4. PPARα agonist suppressed TLR4 expression and inhibited TLR4 signaling. A: ARPE 19 cells at confluence of 90% were transfected with 1 μg plasmid DNA containing a SEAP reporter gene under controlling by NF-κB/AP-1. The same amount control vector served as negative control. Forty-eight hours after reaching the acquiescence in the freshly prepared medium, the cells were exposed to 1 μg/ml LPS in the absence or presence of 50 μM fenofibrate for 24 h. The NF-κB transcriptional activity was measured by SEAP activity. B: The C3H/TLR4 mutant reporter cells with stably expressed NF-κB were exposed to 1 μg/ml LPS or 100 μg/ml of Pam3CSK4 for 24 h, the NF-κB transcriptional activity was measured by SEAP activity. C & D: At confluence, the C3H/TLR4mut reporter cells were exposed with or without 100 μg/ml of Pam3CSK4 or 1 μg/ml of LPS in the presence of 50 μM fenofibrate for 24 h. The NF-κB transcriptional activity was determined by SEAP activity. E: The reporter cells with stably expressed TLR4/MD-2/NF-κB were cultured in the presence of fenofibrate at doses of 0, 25, 50 and 100 μM for 24 h and then exposed to 1 μg/ml LPS for 1 h. The NF-κB transcriptional activity indicating the SEAP activity was measured (mean ± SD, $n = 5$, ###$p < 0.01$ vs. control without LPS; ***$p < 0.001$ vs. LPS). F & G: Representative Western blot analysis of TLR4 levels in the iris of normal rats, EIU rats, and EIU rats pre-treated with fenofibrate. The TLR4 levels were semi-quantified by densitometry and normalized by β-actin levels (mean ± SD, $n = 3$, ***$p < 0.001$). H & I: Western blot analysis of TLR4 levels in control ARPE19 cells, and ARPE19 cells exposed to LPS in the presence with/without fenofibrate. The TLR4 levels were semi-quantified by densitometry and normalized by β-actin levels (mean ± SD, $n = 3$, ***$p < 0.001$). J: Representative immunocytochemical staining of TLR4 and NF-κB in RPE cells. Scale bar: 20 μm in large images and 50 μm in small images.

an eight-fold increase in TLR4 signaling, as evidenced by SEAP activity, which was markedly reduced in response to fenofibrate treatment (Fig. 4A). In 293T reporter cells, which stably co-express the human TLR4/MD-2/CD14 gene and NF-κB/AP1-inducible SEAP reporter gene, LPS stimulation induced a similar increase in NF-κB signaling, whereas this increase was partially reduced following treatment with fenofibrate (Fig. 4B–D). However, increased fenofibrate concentrations did not result in dose-dependent reductions in NF-κB signaling in stable reporter cells (Fig. 4E), indicating that fenofibrate likely inhibits TLR4/NF-κB signaling via effects on upstream pathway components. To address this possibility, we examined TLR4 levels in the uveas of EIU rats and in ARPE19 cells by Western blot analysis. In EIU rats, LPS challenge resulted in a remarkable increase in the levels of TLR4 in the iris, whereas greater than 60% of this increase was reduced by treatment with fenofibrate (Fig. 4F and G). Similarly, exposure to LPS induced a two-fold increase in TLR4 expression compared to the control, whereas the presence of fenofibrate returned TLR4 expression to the basal level in ARPE19 cells (Fig. 4H and I).

Immunocytochemistry revealed that TLR4 signaling was remarkably increased and shifted from the cell surface to the cytoplasm following LPS stimulation, which were completely reversed in response to fenofibrate treatment. Consistently, exposure to LPS induced NF-κB nuclear translocation which was inhibited by fenofibrate (Fig. 4J). These results suggested that fenofibrate inhibited TLR4/NF-κB signaling likely through down-regulating TLR4.

3.4. PPARα agonist treatment ameliorated inflammation and inhibited TLR4/NF-κB signaling in a PPARα-dependent manner

PPARα is abundant in the liver, and in PPARα knockout mice, the hepatic PPARα was shown with a complete cleanup (Supplemental Fig. 3). To determine whether the presence of PPARα is essential for inhibition of TLR4 and inflammatory cytokine production, we established a parallel study in primary liver cells cultured from wild-type (wt) or *Pparα*$^{-/-}$ mice. Compared to wt cells, the absence of PPARα substantially increased the expression of TLR4, TNF-α and VEGF in these primary cells (Fig. 5), suggesting that PPARα is required for the activation of TLR4 signaling.

We next sought to determine whether fenofibrate down-regulates TLR4 and decreases pro-inflammatory cytokine production via PPARα activation. We examined the effects of WY14643, another PPARα-specific agonist, on TLR4 levels, NF-κB activation, and pro-inflammatory factor production in APRE 19 cells. Compared to the controls, exposure of RPE cells to LPS significantly increased the cellular levels of phosphorylated NF-κB, TNF-α, and VEGF and the increases were reduced by fenofibrate or WY14643 (50 μM) to a level comparable to the controls (Fig. 6A). In contrast, co-application of fenofibrate and GW6471, a PPARα-specific antagonist, abolished the inhibitory effects of fenofibrate on the levels of cellular phosphorylated NF-κB (Fig. 6B), TNF-α (Fig. 6C), and VEGF (Fig. 6D), indicating that fenofibrate reduced the LPS-induced production of inflammatory cytokines via PPARα activation. TLR4/NF-κB signaling was further assessed by staining RPE cells with antibodies against TLR4/NF-κB, and the results indicated that LPS stimulation markedly increased TLR4 signaling and induced NF-κB nuclear translocation, both of which were completely inhibited by WY14643. Moreover, the co-application of Wy14643 and GW6471 abolished the inhibitory effects of Wy14643 on LPS-induced TLR4/NF-κB activity (Fig. 6E). Taken together, these results suggest that PPARα activation negatively regulates the TLR4/NF-κB pathway.

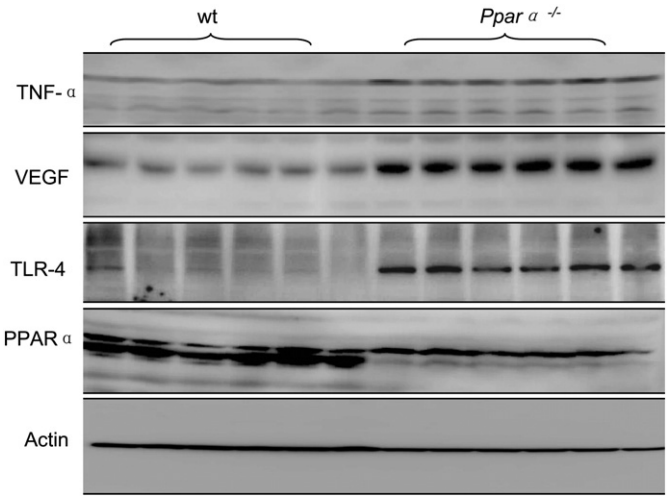

Fig. 5. Deletion of PPARα increased TLR4 and inflammatory cytokine expressions. The cellular levels of TNF-α, VEGF, and TLR4 in primary cultured liver cells from wt mice and *Pparα*$^{-/-}$ mice were determined by Western blot analysis.

3.5. PPARα activation negatively regulated TLR4 gene transcriptional activity

Because PPARα-mediated down-regulation of TLR4 could be caused by transcriptional inhibition of the TLR4 gene or by an increase in TLR4 protein degradation, we examined the effects of PPARα activation on TLR4 mRNA levels in both in vivo and in vitro models. LPS resulted in a greater than 20-fold increase in TLR4 mRNA levels in the irises of EIU rats, whereas feeding with fenofibrate completely prevented the increase in TLR4 expression during EIU (Fig. 7A). Consistently, LPS stimulation resulted in an eight-fold increase in TLR4 expression in RPE cells, which was fully returned to the basal level following fenofibrate treatment (Fig. 7B). These results suggest that the decrease in TLR4 protein is most likely mediated through PPARα-driven down-regulation of TLR4 gene transcription.

To confirm this, we next examined the promoter transcriptional activity of TLR4 in the presence or absence of PPARα agonists in ARPE19 cells. As shown in Fig. 7C, compared to the controls, presence of fenofibrate or WY14643 significantly decreased the TLR4 promoter activity, indicating that activation of PPARα negatively regulates the TLR4 gene transcription. Because deletion of PPARα gene resulted in TLR4 and inflammatory cytokine elevation in RPE cells, we have also assessed the impact of PPARα gene on the TLR4 gene's transcription. As shown in Fig. 7D, down-regulation of PPARα gene expression by transfection of a vector encoded PPARα shRNA significantly increased the TLR4 transcriptional activity. These results confirm that PPARα gene is a negative regulator for TLR4 transcription.

3.6. LPS antagonized PPARα activation in PPARα reporter cells

Because PPARα was shown to function as a repressor of TLR4 transcription, we next evaluated whether LPS-induced TLR4 expression was mediated through PPARα deactivation. The ability of LPS to affect PPARα activity was assessed using a stable transfection reporter system, which incorporated a cDNA encoding luciferase under control of a gene containing the ligand-binding domain of human PPARα. In this system, the EC_{50} for GW590735, a PPARα agonist, to activate PPARα was 9.8 nM, and the EC_{80} was 20 nM. These stable reporter cells were treated with doses of GW590735 ranging between 0 and 20 nM in the absence or presence of LPS ranging from 0 to 4 μg/ml for 24 h. As shown in Fig. 8A, 4 μg/ml of LPS was able to inhibit GW590735-mediated activation of PPARα by approximately 80%. A dose–response study further showed inhibition levels of ~25, 40, and 70% at doses of 0.5, 1, and 2 μg/ml of LPS, respectively; at doses greater than 8 μg/ml, the toxicity of LPS prevented further measurements.

Likewise, the effects of LPS on PPARα activated by WY14643 and fenofibrate were also investigated in these stable reporter cells. As shown in Fig. 8B, the EC_{50} for activation mediated by Wy14643 was

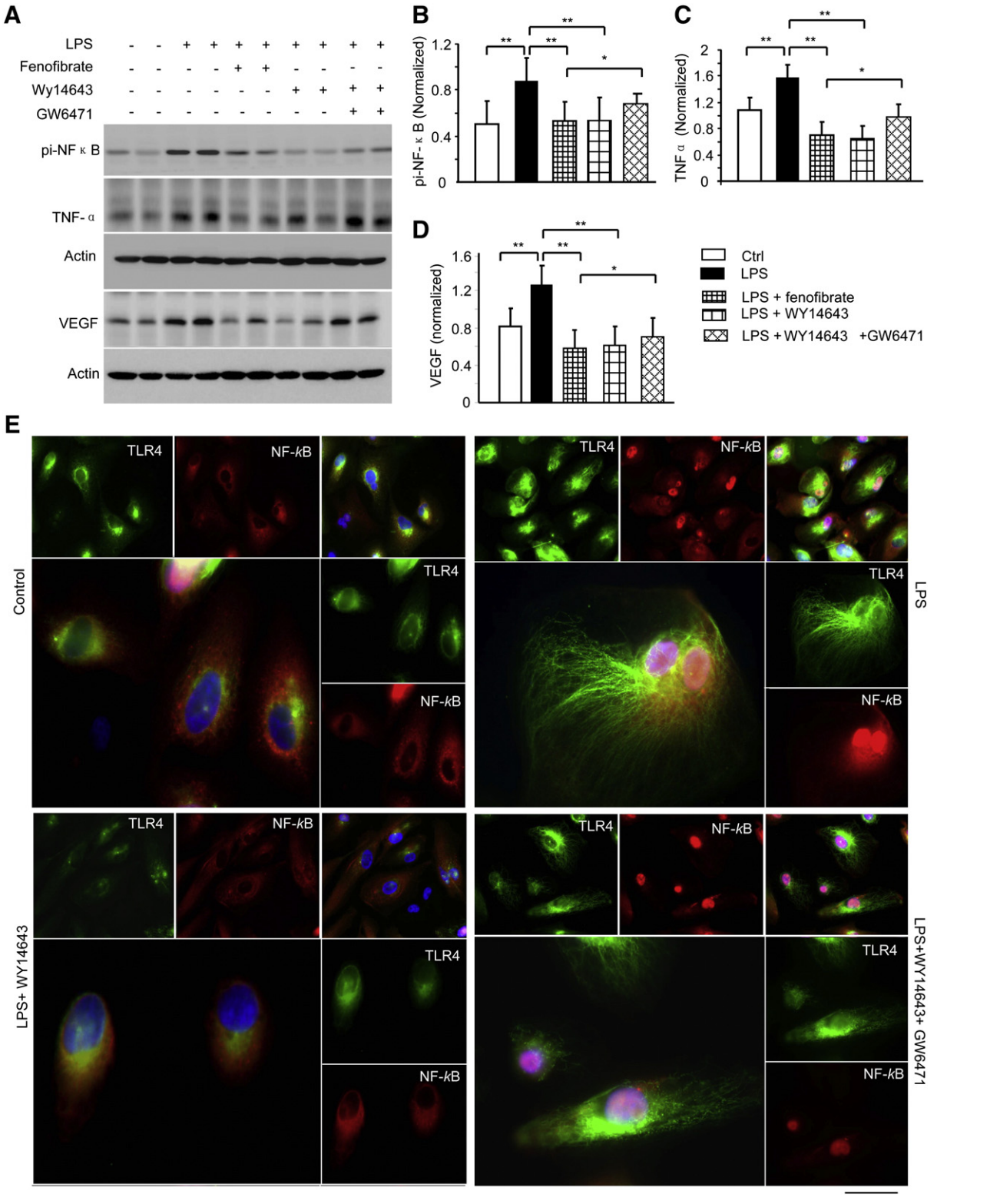

Fig. 6. PPARα agonists reduced inflammatory cytokine production and inhibited TLR4 signaling in a PPARα dependent manner. Confluent ARPE 19 cells were cultured in a medium in the absence or presence of 50 μM fenofibrate or 50 μM WY14643 and/or with 10 μM GW6471 overnight and then exposed to 1 μg/ml LPS for 1 h. A: Representative Western blot analysis of cellular phosphorylated NF-κB, TNF-α and VEGF levels from the same amount of whole cell lysis. B–D: Statistical analysis of phosphorylated NF-κB, TNF-α, VEGF and ICAM-1 levels after being normalized with β-actin (mean ± SD, $n = 3$, $^{*}p < 0.05$, $^{**}p < 0.01$). E: Representative immunocytochemistry of the activation of TLR4/NF-κB signaling. Green: TLR4; Red: NF-κB; Blue, DAPI. Scale bar: 20 μm for large images, 50 μm for small images.

40 μM, and the dose–response study demonstrated that LPS inhibited PPARα activity by ~25, 50, and 70% at doses of 0.5, 1, and 2 μg/ml, respectively. The EC_{50} for activation mediated by fenofibrate was approximately 30 μM, and the dose–response study demonstrated similar findings as that for WY14643 (Fig. 8C), indicating that the effect of LPS-mediated inhibition of PPARα was specific and that LPS could demonstrate PPARα antagonist properties. These results suggest that LPS induced TLR level may through inhibition of PPARα.

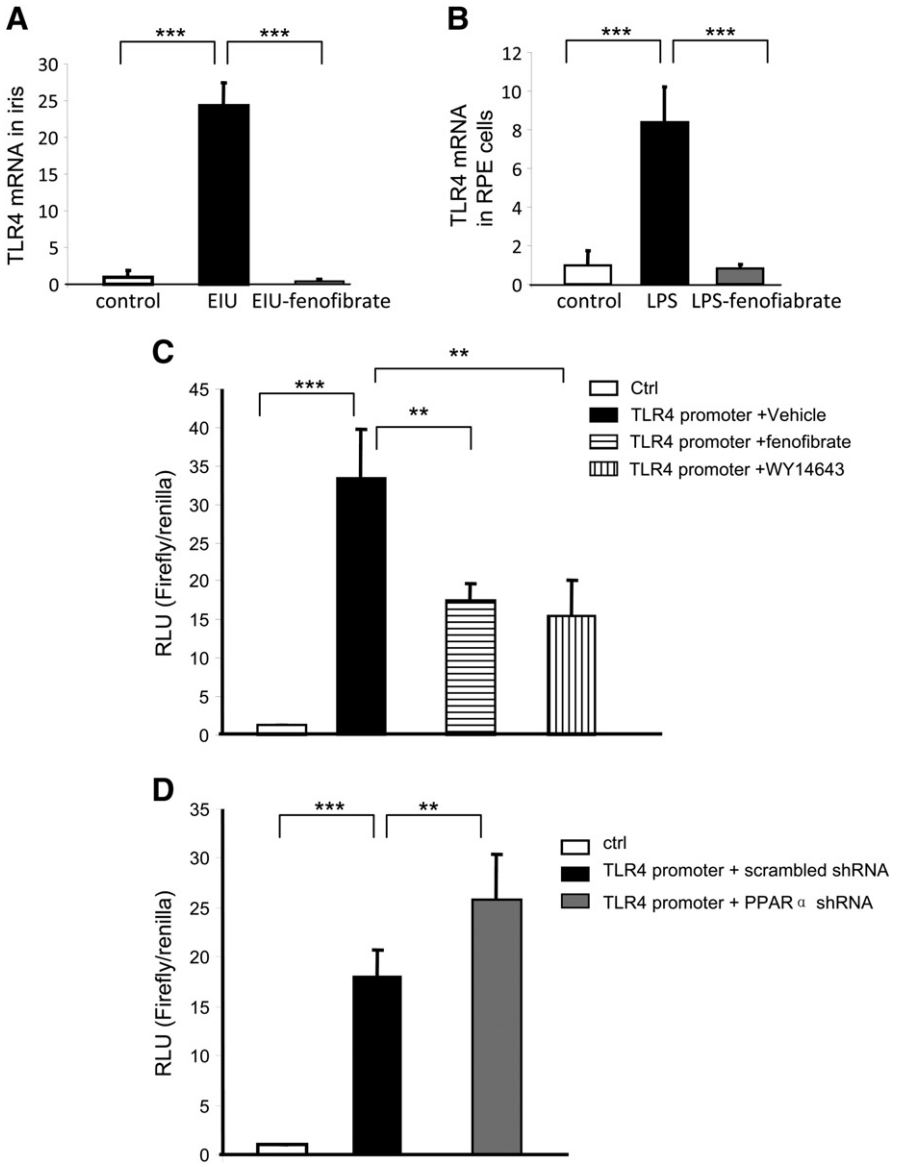

Fig. 7. Activation of PPARα down-regulated TLR transcriptional activity. A: TLR4 mRNA levels in the eyecups from normal rats, EIU rats, and EIU rats pre-treated with fenofibrate were determined by real-time PCR and normalized by 18*S* RNA (mean ± SD, $n = 3$, $^{**}p < 0.05$, $^{***}p < 0.001$). B: ARPE 19 cells at confluence were exposed to normal medium; a medium containing 1 μg/ml LPS in the absence or presence of fenofibrate. TLR4 mRNA levels from each group were determined by real-time PCR analysis and normalized by 18*S* RNA (mean ± SD, $n = 3$, $^{**}p < 0.05$, $^{***}p < 0.001$). C: Confluent ARPE 19 cells were co-transfected with vectors containing of TLR4 promoter and PRL-TK. Twenty-four hours after achieving quiescence in a freshly prepared medium, the cells were exposed to a cultured medium in the presence or absence of fenofibrate (50 μM) or WY14643 (50 μM) for 16 h, the same amount vehicle served as control. TLR4 transcriptional activity was determined by luciferase assay and normalized by Renilla luciferase activity (mean ± SD, $n = 3$, $^{**}p < 0.05$, $^{***}p < 0.001$). D: Confluent ARPE 19 cells were transfected with plasmids of TLR4 promoter, PPARα ShRNA, and PRL-TK (to normalize the transfection efficiency). The transcriptional activity of TLR4 promoter was determined by luciferase assay and normalized by Renilla luciferase activity (mean ± SD, $n = 3$, $^{**}p < 0.01$, $^{***}p < 0.001$).

4. Discussion

The exact role of PPARα in regulating TLR4 signaling was unclear. The results presented here suggest that activation of PPARα decreases TLR4 levels and inhibits the NF-κB signaling pathway through suppression of TLR4 transcriptional activity, representing a new therapeutic mechanism for the treatment of uveitis.

PPARα regulates and interacts with a diverse group of molecules. PPARα activation was reported to inhibit the NF-κB pathway and consequently results in the reduction of the inflammatory factors COX2, IL1, and TNF-α. But it was unclear how PPARα activation inhibits NF-κB pathway. One explanation is that activation of PPARα inhibition of the NF-κB pathway was through ligand-dependent trans-repression, while another study suggested that this inhibition is through increased expression of Iκa. However, it is still unclear whether up-regulation of Iκa expression is associated with the TLR pathway. The data presented in this study suggest that the ability of PPARα to down-regulate TLR4 transcription plays a central role in the regulation of its down-stream pathway. Thus application of PPARα agonists in the treatment of TLR related inflammation diseases is theoretically practicable.

Present studies of fenofibrate's therapeutic effects on EAU models (Supplemental Fig. 2A) bear out this feasibility as the presence of MyD88 is essential for EAU induction [20,21]. In addition to providing the evidence that activation of PPARα prevents EAU, our results also showed that the TLR4 levels were down-regulated in EAU models (Supplemental Fig. 2B). Interestingly, a recent study done by Okunuki et al. showed a similar result that activation of PPARγ by pioglitazone has a rescue effect on an EAU model by suppressing the productions of inflammatory cytokines of TNF-α and IL6 [22]. Although the study didn't mention if this inhibition was through down-regulation of TLR transcription by PPARγ, evidences in various diseases and cells support this possibility [23,24]. On the other hand, in addition to be a PPARγ

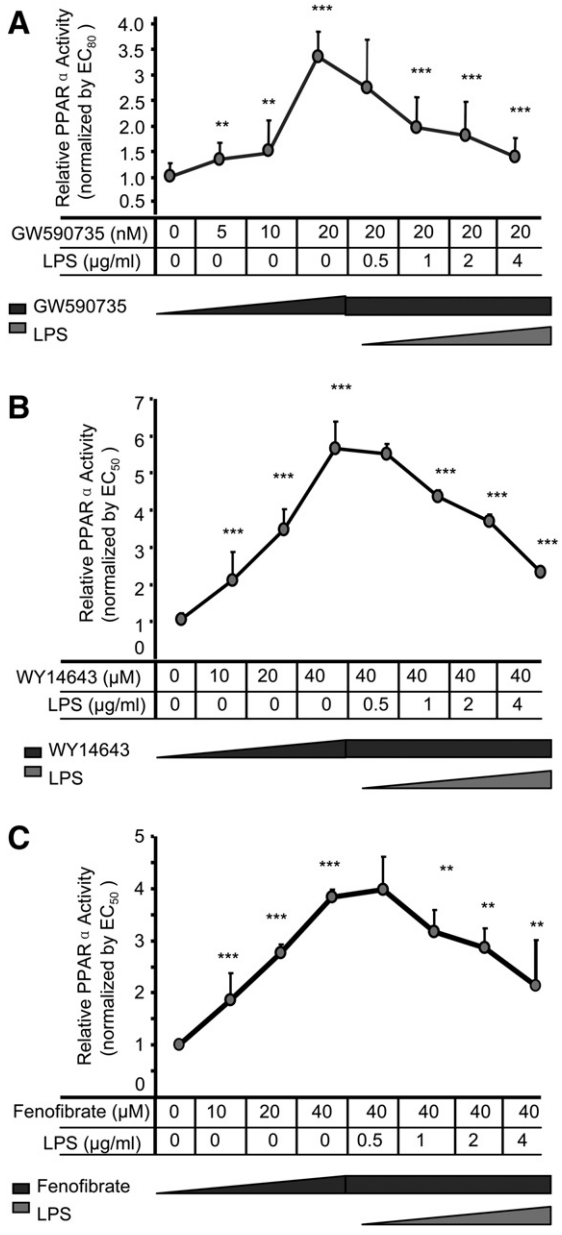

Fig. 8. LPS antagonized PPARα activation in PPARα reporter cells. A–C: The PPARα ligand-activation effective concentration values of GW590735, WY14643, and fenofibrate were confirmed in the reporter cells at doses of 20 nM, 40 μM, and 40 μM, respectively. Confluenced PPARα reporter cells were cultured in a medium containing 20 nM GW590735 (A), 40 μM WY14643 (B), and 40 μM fenofibrate (C), respectively, in the presence of a range of LPS at 0–4 μg/ml overnight. The luciferase activities were measured using a luminometer (mean ± SD, $n = 4$, $^{*}p < 0.05$, $^{**}p < 0.01$, $^{***}p < 0.001$).

activator, pioglitazone seems to act like a partial stimulator for PPARα [25]. Therefore it is unclear if pioglitazone suppresses TLR4 transcription through activation of PPAR-α, even at a lesser extent. Besides the anti-uveitis functions, PPARα and PPARγ have the similar capability of anti-inflammation in other diseases. For example, in type 1 diabetic model, activation of PPARγ by rosiglitazone reduced the expression of ICAM-1 and suppressed retinal leukostasis [26], a similar phenomenon which we reported previously but with fenofibrate activation of PPARα [14]. Meanwhile, the expressions of PPARγ and PPARα are very interesting. Both PPARγ and PPARα are abundant in human RPE cells, where TLR4 is expressed (Supplemental Fig. 1). Therefore it is possible that the genes regulated by PPARγ and PPARα in the RPE cells interact and cooperate, however, the mechanism for the TLR4 down-regulation in RPE cells still requires further study.

In addition to the aforementioned anti-inflammatory functions, the most studied role of PPARα is regulating a number of genes involved in free fatty acid (FFA) metabolism and insulin resistance. FFAs are known to mediate inflammation and are believed to contribute to insulin resistance. The effects of PPARα on FFAs' activity include the up-regulated expression of genes involved in the transportation and oxidation of FFAs, which reduce de novo FFA synthesis. Recently, several plausible studies have revealed the ability of FFAs to stimulate TLR4-dependent inflammatory pathways. For example, FFAs act as direct ligands for TLR4, and they indirectly activate the TLR4 pathway through binding to the adaptor protein Fetuin-A [27,28]. In addition to these actions, FFAs have also been shown to promote the accumulation and homodimerization of TLR4 in the cell membrane, leading to activation of the TLR4 pathway [29]. Although our study demonstrates that PPARα activation inhibits TLR4 transcription, it is unclear whether this TLR4 inhibition is associated with the reduction effects of PPARα on FFA production.

The inhibitory effect of LPS on PPARα was previously unknown. In a cell-based reporter assay, we found that LPS is a PPARα antagonist. The binding of LPS to PPARα reduced PPARα activity, which contributed, at least partially, to the effects of LPS-induced TLR4 signaling. This finding also verified that PPARα negatively regulates the TLR4 signaling, although the precise mechanism by which LPS inhibits the PPARα activation remains unclear. An analysis of the structure of LPS shows that LPS mainly consists of a polysaccharide region and an endotoxin, a specific carbohydrate lipid moiety termed lipid A, which is responsible for the immunostimulatory activity of LPS. Crystal structure analysis of PPARα agonists and antagonists revealed that a hydrogen bonded interaction between the carboxylic acid group of a PPARα agonist and Y464 on the C-terminal AF-2 helix of PPARα stabilized the receptor and the active confirmation change [30]. Normally, nuclear transcription repression of gene transcription is mediated through interactions with co-repressor proteins such as SMRT and N-CoR [31,32], which subsequently recruits histone deacetylases to the chromatin [33,34]. One example is the PPARα antagonist GW6471, as a PPARα LBD bound to GW6471 at a SMRT co-repressor motif led to SMRT motif structural changes and prevented activation of functional conformation [30]. However, whether this mechanism applies to the interaction between LPS and PPARα and whether the presence of a PPARα agonist interrupts the binding of LPS to TLR4 remain unclear, further biochemical analyses and structure-based mutagenesis of LPS might provide additional information. Overall, our current study suggests that PPARα activation has the novel function of negatively regulating TLR4 signaling, which could represent a new therapeutic strategy for the treatment of inflammatory diseases.

Supplementary data to this article can be found online at http://dx.doi.org/10.1016/j.bbadis.2014.03.015.

Conflicts of interest

The authors have declared that no conflict of interest exists.

Acknowledgements

This work is supported by the research awards from ADA (7-11-JF-10), JDRF (5-2013-58), a grant P20RR024215 from the National Center for Research Resources, and the Fundamental Research Funds of State Laboratory of Ophthalmology.

References

[1] K. Tabeta, P. Georgel, E. Janssen, X. Du, K. Hoebe, K. Crozat, S. Mudd, L. Shamel, S. Sovath, J. Goode, L. Alexopoulou, R.A. Flavell, B. Beutler, Toll-like receptors 9 and 3 as essential components of innate immune defense against mouse cytomegalovirus infection, Proc. Natl. Acad. Sci. U. S. A. 101 (2004) 3516–3521.

[2] B. Beutler, K. Hoebe, L. Shamel, Forward genetic dissection of afferent immunity: the role of TIR adapter proteins in innate and adaptive immune responses, C. R. Biol. 327 (2004) 571–580.
[3] R. Medzhitov, P. Preston-Hurlburt, C.A. Janeway Jr., A human homologue of the *Drosophila* Toll protein signals activation of adaptive immunity, Nature 388 (1997) 394–397.
[4] A. Poltorak, X. He, I. Smirnova, M.Y. Liu, C. Van Huffel, X. Du, D. Birdwell, E. Alejos, M. Silva, C. Galanos, M. Freudenberg, P. Ricciardi-Castagnoli, B. Layton, B. Beutler, Defective LPS signaling in C3H/HeJ and C57BL/10ScCr mice: mutations in Tlr4 gene, Science 282 (1998) 2085–2088.
[5] M.W. Hornef, B.H. Normark, A. Vandewalle, S. Normark, Intracellular recognition of lipopolysaccharide by Toll-like receptor 4 in intestinal epithelial cells, J. Exp. Med. 198 (2003) 1225–1235.
[6] F. Backhed, M. Hornef, Toll-like receptor 4-mediated signaling by epithelial surfaces: necessity or threat? Microbes Infect. 5 (2003) 951–959.
[7] J.T. Rosenbaum, H.O. McDevitt, R.B. Guss, P.R. Egbert, Endotoxin-induced uveitis in rats as a model for human disease, Nature 286 (1980) 611–613.
[8] C.G. Espiritu, R. Gelber, H.B. Ostler, Chronic anterior uveitis in leprosy: an insidious cause of blindness, Br. J. Ophthalmol. 75 (1991) 273–275.
[9] M.J. Ronday, J.S. Stilma, R.F. Barbe, A. Kijlstra, A. Rothova, Blindness from uveitis in a hospital population in Sierra Leone, Br. J. Ophthalmol. 78 (1994) 690–693.
[10] D.F. Shen, R.R. Buggage, H.C. Eng, C.C. Chan, Cytokine gene expression in different strains of mice with endotoxin-induced uveitis (EIU), Ocul. Immunol. Inflamm. 8 (2000) 221–225.
[11] J. Mathison, E. Wolfson, S. Steinemann, P. Tobias, R. Ulevitch, Lipopolysaccharide (LPS) recognition in macrophages. Participation of LPS-binding protein and CD14 in LPS-induced adaptation in rabbit peritoneal exudate macrophages, J. Clin. Invest. 92 (1993) 2053–2059.
[12] Q. Li, B. Peng, S.M. Whitcup, S.U. Jang, C.C. Chan, Endotoxin induced uveitis in the mouse: susceptibility and genetic control, Exp. Eye Res. 61 (1995) 629–632.
[13] I.E. Elijah, E. Borsheim, D.M. Maybauer, C.C. Finnerty, D.N. Herndon, M.O. Maybauer, Role of the PPAR-alpha agonist fenofibrate in severe pediatric burn, Burns 38 (2012) 481–486.
[14] Y. Chen, Y. Hu, M. Lin, A.J. Jenkins, A.C. Keech, R. Mott, T.J. Lyons, J.X. Ma, Therapeutic effects of PPARalpha agonists on diabetic retinopathy in type 1 diabetes models, Diabetes 62 (2013) 261–272.
[15] R. Krysiak, A. Gdula-Dymek, B. Okopien, Effect of simvastatin and fenofibrate on cytokine release and systemic inflammation in type 2 diabetes mellitus with mixed dyslipidemia, Am. J. Cardiol. 107 (2011) 1010–1018 (e1011).
[16] R. Krysiak, A. Gdula-Dymek, B. Okopien, The effect of fenofibrate on lymphocyte release of proinflammatory cytokines and systemic inflammation in simvastatin-treated patients with atherosclerosis and early glucose metabolism disturbances, Basic Clin. Pharmacol. Toxicol. 112 (2013) 198–202.
[17] E.T. Price, G.J. Welder, I. Zineh, Modulatory effect of fenofibrate on endothelial production of neutrophil chemokines IL-8 and ENA-78, Cardiovasc. Drugs Ther. 26 (2012) 95–99.
[18] I. Pouvreau, J.C. Zech, B. Thillaye-Goldenberg, M.C. Naud, N. Van Rooijen, Y. de Kozak, Effect of macrophage depletion by liposomes containing dichloromethylene-diphosphonate on endotoxin-induced uveitis, J. Neuroimmunol. 86 (1998) 171–181.
[19] Y. Chen, Y. Hu, K. Lu, J.G. Flannery, J.X. Ma, Very low density lipoprotein receptor, a negative regulator of the wnt signaling pathway and choroidal neovascularization, J. Biol. Chem. 282 (2007) 34420–34428.
[20] S. Saraswathy, A.M. Nguyen, N.A. Rao, The role of TLR4 in photoreceptor {alpha}a crystalline upregulation during early experimental autoimmune uveitis, Invest. Ophthalmol. Vis. Sci. 51 (2010) 3680–3686.
[21] S.B. Su, P.B. Silver, R.S. Grajewski, R.K. Agarwal, J. Tang, C.C. Chan, R.R. Caspi, Essential role of the MyD88 pathway, but nonessential roles of TLRs 2, 4, and 9, in the adjuvant effect promoting Th1-mediated autoimmunity, J. Immunol. 175 (2005) 6303–6310.
[22] Y. Okunuki, Y. Usui, H. Nakagawa, K. Tajima, R. Matsuda, S. Ueda, T. Hattori, T. Kezuka, H. Goto, Peroxisome proliferator-activated receptor-gamma agonist pioglitazone suppresses experimental autoimmune uveitis, Exp. Eye Res. 116 (2013) 291–297.
[23] Y. Yin, G. Hou, E. Li, Q. Wang, J. Kang, PPAR gamma agonists regulate tobacco smoke-induced Toll like receptor 4 expression in alveolar macrophages, Respir. Res. 15 (2014) 28.
[24] K. Hu, Y. Yang, Q. Tu, Y. Luo, R. Ma, Alpinetin inhibits LPS-induced inflammatory mediator response by activating PPAR-gamma in THP-1-derived macrophages, Eur. J. Pharmacol. 721 (2013) 96–102.
[25] J. Sakamoto, H. Kimura, S. Moriyama, H. Odaka, Y. Momose, Y. Sugiyama, H. Sawada, Activation of human peroxisome proliferator-activated receptor (PPAR) subtypes by pioglitazone, Biochem. Biophys. Res. Commun. 278 (2000) 704–711.
[26] K. Muranaka, Y. Yanagi, Y. Tamaki, T. Usui, N. Kubota, A. Iriyama, Y. Terauchi, T. Kadowaki, M. Araie, Effects of peroxisome proliferator-activated receptor gamma and its ligand on blood–retinal barrier in a streptozotocin-induced diabetic model, Invest. Ophthalmol. Vis. Sci. 47 (2006) 4547–4552.
[27] H. Shi, M.V. Kokoeva, K. Inouye, I. Tzameli, H. Yin, J.S. Flier, TLR4 links innate immunity and fatty acid-induced insulin resistance, J. Clin. Invest. 116 (2006) 3015–3025.
[28] D. Pal, S. Dasgupta, R. Kundu, S. Maitra, G. Das, S. Mukhopadhyay, S. Ray, S.S. Majumdar, S. Bhattacharya, Fetuin-A acts as an endogenous ligand of TLR4 to promote lipid-induced insulin resistance, Nat. Med. 18 (2012) 1279–1285.
[29] S.W. Wong, M.J. Kwon, A.M. Choi, H.P. Kim, K. Nakahira, D.H. Hwang, Fatty acids modulate Toll-like receptor 4 activation through regulation of receptor dimerization and recruitment into lipid rafts in a reactive oxygen species-dependent manner, J. Biol. Chem. 284 (2009) 27384–27392.
[30] H.E. Xu, T.B. Stanley, V.G. Montana, M.H. Lambert, B.G. Shearer, J.E. Cobb, D.D. McKee, C.M. Galardi, K.D. Plunket, R.T. Nolte, D.J. Parks, J.T. Moore, S.A. Kliewer, T.M. Willson, J.B. Stimmel, Structural basis for antagonist-mediated recruitment of nuclear co-repressors by PPARalpha, Nature 415 (2002) 813–817.
[31] A.J. Horlein, A.M. Naar, T. Heinzel, J. Torchia, B. Gloss, R. Kurokawa, A. Ryan, Y. Kamei, M. Soderstrom, C.K. Glass, et al., Ligand-independent repression by the thyroid hormone receptor mediated by a nuclear receptor co-repressor, Nature 377 (1995) 397–404.
[32] J.D. Chen, R.M. Evans, A transcriptional co-repressor that interacts with nuclear hormone receptors, Nature 377 (1995) 454–457.
[33] L. Nagy, H.Y. Kao, D. Chakravarti, R.J. Lin, C.A. Hassig, D.E. Ayer, S.L. Schreiber, R.M. Evans, Nuclear receptor repression mediated by a complex containing SMRT, mSin3A, and histone deacetylase, Cell 89 (1997) 373–380.
[34] C.D. Laherty, W.M. Yang, J.M. Sun, J.R. Davie, E. Seto, R.N. Eisenman, Histone deacetylases associated with the mSin3 corepressor mediate mad transcriptional repression, Cell 89 (1997) 349–356